

Disentangling the Delayed-Choice Quantum Eraser

Thomas V. Higgins

Abstract

This paper examines the experimental setup and physics behind the delayed-choice quantum eraser and offers the simplifying metaphor of a game of chance played with entangled dice. The paper takes the reader step-by-step through the experiment and the physics governing each element of it. A general undergraduate familiarity with quantum mechanics is assumed.

Published by tvhiggins.com March 27, 2025

Introduction

Perhaps the most insightful declaration ever made about quantum mechanics came from one of its most important contributors, Richard P. Feynman, who once proclaimed, “Nobody understands quantum mechanics.” Despite being the most successful theory about the physical universe ever conceived by humankind, nobody can truthfully claim that it makes total sense to them, because it just doesn’t. Plus, the more we learn about quantum theory, and the more sophisticated our experiments become, the stranger it gets.

Such is the case with the now famous delayed-choice quantum eraser experiment, which was first described by Kim and others in 2000. [\[1\]](#) Since then, many have attempted to interpret and explain its results. Some interpretations are more lucid than others [\[2\]](#) [\[3\]](#) [\[4\]](#), but in many cases the experiment seems to engender more confusion than clarity, especially in articles written for the general audience. Chief among these misinterpretations is the notion that the experiment proves that the present can affect the past—so-called “retrocausality.” Color me doubtful about this one. If the present could affect the past, there are a few things I’d like to undo. But I personally don’t think it’s possible. Who knows, though, maybe one day someone will prove me wrong about that, too. Nobody really understands quantum mechanics. Nonetheless, this paper offers yet another attempt to explain what might be going on in the delayed-choice quantum eraser.

Young’s double-slit experiment with a pivotal quantum twist

Figure 1 shows the basic setup of the original experiment. At the bottom of the figure, UV light (351.1-nm) from an argon-ion laser (blue arrows) irradiates a double slit, just like in Young’s classic experiment. However, the similarity to Young’s experiment quickly vanishes next, because the wavefunction of each coherent UV photon that passes through the two slits is used to pump two regions (1 and 2 in Figure 1) of a β -Barium Borate (BBO) crystal. Understanding what happens next within this nonlinear crystal is a key to understanding how the experiment works, because that’s where much of the quantum magic happens.

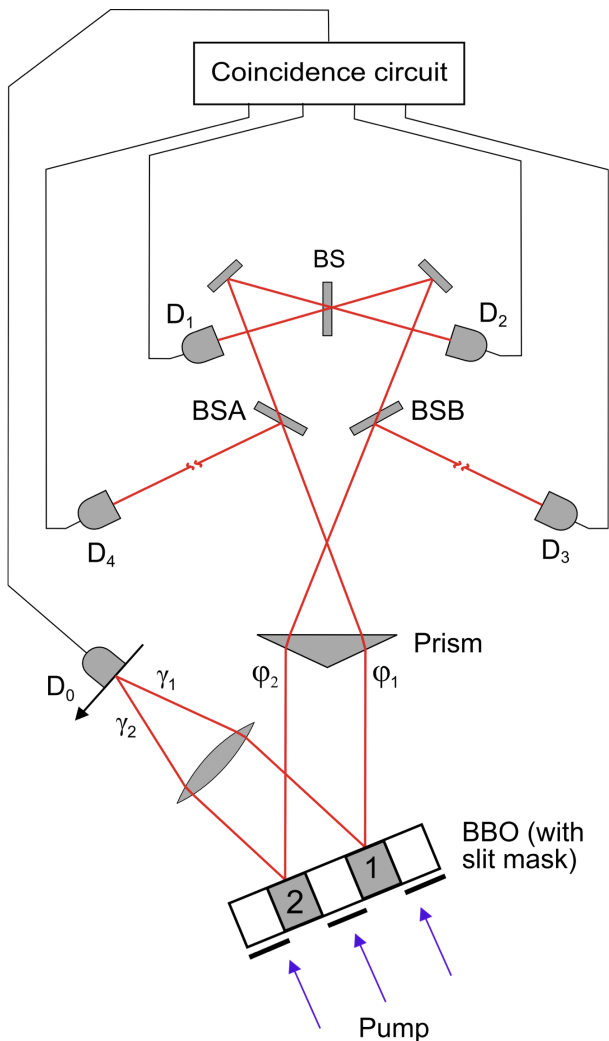


Figure 1

experiment, the BBO crystal has a thickness within which SPDC takes place. Kim et al. used a 0.3-mm-thick crystal in their original experiment. This would ordinarily scramble the phases of wavefronts emerging from the crystal if it weren't for another very important condition: phase matching.

In my opinion, the phase-matching condition is the most important SPDC property in this experiment next to entanglement. Even so, most explanations of the delayed-choice quantum eraser that I've read fail to even mention it.

Most of the pumping photons just pass right through the BBO crystal. Type-II spontaneous parametric down conversion, or SPDC for short, is a very inefficient process. But each pump photon of a lucky few (1 in 10^6) will be transformed within the crystal into two new photons having twice the wavelength (702.2 nm) and therefore half the frequency or energy.

Now, there are a few important details to recognize about SPDC. First, down conversion is a non-local quantum process, meaning that both regions of the crystal participate in the creation of each photon pair from each pump photon. Consequently, you can't know which region a down-converted photon pair came from: region 1, region 2, or both. In this regard, the quantum physics mimics the classic double-slit experiment.

Second, unlike the double-slit

The phase-matching condition follows naturally from the conservation laws, whereby the sum of the energy (or the momentum) of the two down-converted photons (signal γ and idler ϕ in Figure 1) must equal the energy (or momentum) of the pump photon. Mathematically this is expressed as:

$$\mathbf{k}_p = \mathbf{k}_s + \mathbf{k}_i \quad \text{Eq. 1}$$

$$\omega_p = \omega_s + \omega_i, \quad \text{Eq. 2}$$

where \mathbf{k}_p , \mathbf{k}_s , and \mathbf{k}_i represent the wavevectors of the pump, signal, and idler photons, respectively, and ω_p , ω_s , and ω_i represent their respective angular frequencies. The wavevectors \mathbf{k}_α ($\alpha = p, s, i$) directly express the photons' momenta through the de Broglie relation $\mathbf{p}_\alpha = \hbar \mathbf{k}_\alpha / 2\pi$, and ω_α relates to the photons' energies through Planck's relation $E_\alpha = \hbar \omega_\alpha / 2\pi$ (\hbar = Planck's constant). The phase velocities (\mathbf{v}_α) of pump, signal, and idler also are linked by $\mathbf{v}_\alpha = \omega_\alpha / \mathbf{k}_\alpha$, which lets us to rewrite Eq. 1 as $\omega_p / \mathbf{v}_p = \omega_s / \mathbf{v}_s + \omega_i / \mathbf{v}_i$. Therefore, phase velocities must match the pump, too.

These factors and others—such as refractive indexes along the birefringent crystal axes, polarizations, and temperature—govern the phase matching condition. But the bottom line is that signal and idler must stay in-phase with the pump laser's coherent wavefront as they propagate through the crystal. If their phase sum is not equal to the pump, the SPDC efficiency suffers greatly.

Last but not least, there are three other significant attributes of Type-II SPDC to mention: 1) the pump photon creates the signal/idler pair simultaneously, 2) signal and idler polarization states are mutually orthogonal, and 3) the signal/idler wavefunction is entangled. This entangled-pair state is described in Dirac notation as: $1/\sqrt{2} (|\Psi_{\gamma H}\rangle|\Psi_{\phi V}\rangle + |\Psi_{\gamma V}\rangle|\Psi_{\phi H}\rangle)$, where $|\Psi_{\gamma H}\rangle|\Psi_{\phi V}\rangle$ denotes the tensor product $\Psi_{\gamma H} \otimes \Psi_{\phi V}$, and subscripts γH , ϕV and γV , ϕH denote horizontally and vertically polarized signal/idler pairs from the BBO. Entanglement basically links two wavefunctions together as one across space and time. Therefore, what you do to one immediately affects the other, no matter how far apart they may get. They are correlated throughout spacetime. Einstein, who was famously bothered by quantum entanglement, called it “spooky action at a distance.” And it is just that—spooky.

The remaining experimental setup

Let's dissect what's going on in the rest of the delayed-choice-quantum-eraser setup. Signal photons (γ) emitted from the two BBO regions are directed off to the left in Figure 1, where they encounter a lens that focuses them onto the scanning detector D_0 . This detector measures the total detection rates of signal photons along the focal plane where the two paths (γ_1 and γ_2) intersect.

Idler photons (ϕ) exit the BBO to a separate area of the setup in Figure 1, where they encounter a prism, three beamsplitters (BSA, BSB, BS), two mirrors, and four detectors (D_1 , D_2 , D_3 , D_4). Optical path lengths from the BBO to these four detectors D_ϕ ($\phi = 1-4$) are all made equal, but they also are intentionally made longer than the optical path length from the BBO to D_0 . This creates a time delay between the detections of each idler photon and its entangled signal-photon twin. In the original experiment, this delay amounts to "at least 8 ns."

Each of the D_ϕ detectors is also electronically linked with D_0 for coincidence detection (see Figure 1 again). Since each signal/idler pair is created simultaneously, coincidence detections will generate a ledger containing four subsets of synchronized event data. Each detection event at D_0 will therefore have a corresponding detection of its entangled twin 8 ns later at one of the D_ϕ detectors.

The experiment in action

Let's now look at what happens when we fire up the laser and start taking data. The first thing to notice on the signal-photon side is that we don't see any interference fringes at D_0 (see Figure 2b). Those who are familiar with the double-slit experiment would expect to see fringes (see Figure 2a), so this may come as a surprise. Let's examine what might be happening here.

The popular explanation for the absence of an interference pattern at D_0 is that entanglement destroys interference. The rationale usually given for this interpretation is that the entangled photons act as tags to one another. This creates the *potential* to determine which-path information, and even the potential for having such information destroys interference.

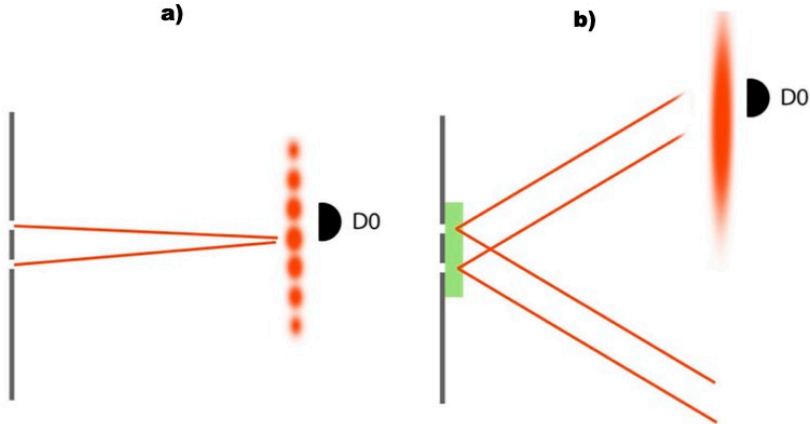


Figure 2 (from [\[2\]](#))

Another viewpoint is that coherence is not so much destroyed by entanglement as it is rendered inaccessible to local measurement; therefore, pure coherent states still can be presumed to exist locally at D_0 , but as an indistinguishable ensemble of mixed states. In this experiment, the states are: region 1 acting alone, region 2 acting alone, regions 1 & 2 acting together in-phase (symmetric), and regions 1 & 2 acting together antiphase (antisymmetric).

In either case, the idler side of the experiment is designed to reconstruct these four pure states from the coincidence-detection data. Here's how that works (refer to Figure 1). Each idler photon emitted from the BBO first encounters the 50/50 beamsplitters BSA and BSB, where there's a 50/50 chance φ_2 will get diverted to D_3 and a 50/50 chance φ_1 will go to D_4 . The purpose here is to glean which-path information about the entangled wavefunction.

Idler wavefunctions that don't get deflected to either D_3 or D_4 proceed via two mirrors to the 50/50 beam splitter BS. The motive of BS is to "erase" which-path information by making it impossible to know which BBO region an entangled idler wavefunction came from. This part of the idler section is called the "quantum eraser" (see Figure 3).

Each idler wavefunction reflected from the two mirrors of the quantum-eraser undergoes a symmetrical phase shift of π -radians, but beam splitter BS imparts a critical asymmetric phase shift. After this beam splitter, each idler wavefunction arriving at D_1 experiences no phase shift between paths φ_1 and φ_2 , while the wavefunction detected at D_2 undergoes a π -radian phase shift between paths φ_1 and φ_2 .

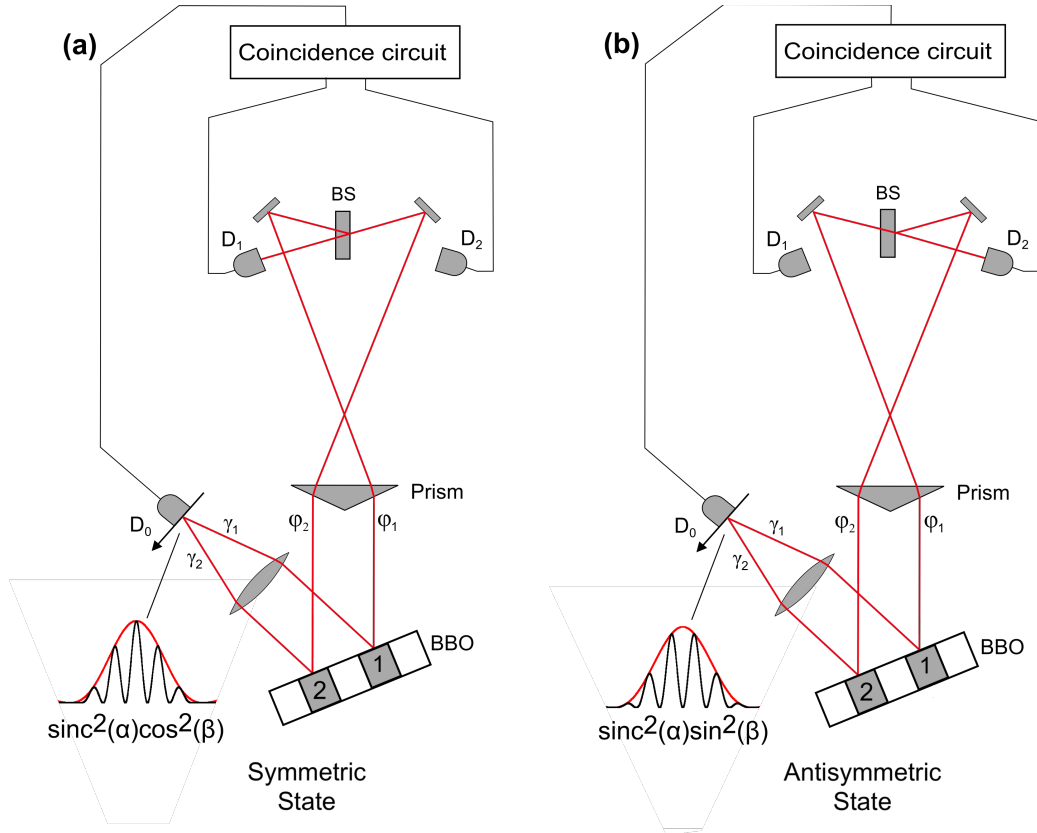


Figure 3

Beamsplitter BS therefore has a very useful sorting capacity. Entangled idler wavefunctions are sorted into a symmetric phase superposition at D_1 (see Figure 3a) and an antisymmetric phase superposition at D_2 (see Figure 3b). The joint signal-idler detection after the quantum eraser therefore can be modeled mathematically as:

$$\Psi = 1/\sqrt{2} [\Psi_{D1} \otimes (-\Psi_{\gamma 1} - \Psi_{\gamma 2})] + 1/\sqrt{2} [\Psi_{D2} \otimes (\Psi_{\gamma 1} - \Psi_{\gamma 2})], \quad \text{Eq. 3} \quad [4]$$

which links the idler (ϕ) detections at D_1 and D_2 to the correlated signal (γ) detections at D_0 , and where the \pm signs within the parentheses convey the *idler's* asymmetric phases at the quantum eraser ($\pm \Psi_{\phi 1} - \Psi_{\phi 2}$) onto its entangled *signal* wavefunction ($\pm \Psi_{\gamma 1} - \Psi_{\gamma 2}$) at D_0 .

Analysis and discussion

Now we can paint a fuller picture of how the delayed-choice quantum eraser works. D_0 - D_1 coincidence detections flag the symmetric state, D_0 - D_2 coincidences flag the antisymmetric state, and D_0 - D_3 or D_0 - D_4 coincidences yield which-path information. So, the delayed-choice quantum eraser acts like a sorting machine. It exploits the tagging feature of entanglement, along with the sorting feature of the quantum eraser, and then combines that information through coincidence detections into accessible coherent wavefunctions.

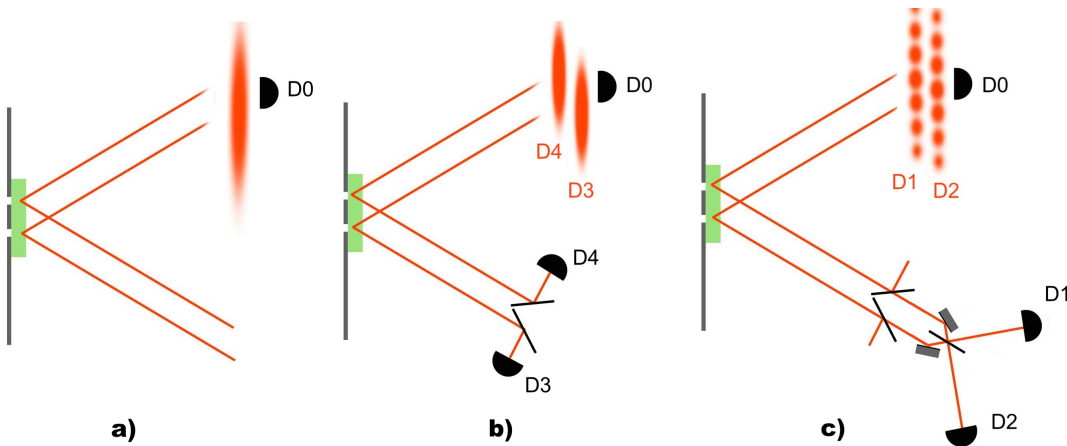


Figure 4 (from [2])

What appears as an incoherent clump pattern at D_0 in Figure 4a is reconstituted by joint signal-idler detections into the coherent pure states of Figures 4b and 4c. Note that when you add together the two states of Figure 4b or 4c, you get the clump distribution locally observed at D_0 (Figure 4a). The complementary symmetric-antisymmetric states shown in Figure 4c are also depicted by the curves drawn in Figures 3a and 3b, respectively. Those curves show how the complementary interference distributions of $\text{sinc}^2 \cos^2$ and $\text{sinc}^2 \sin^2$ (black) add up to a sinc^2 clump distribution (red), as observed at D_0 in the original experiment.

So, in some sense, both reasons given earlier for the lack of interference patterns at D_0 seem reasonable. But in order to “see” the complementary interference patterns of Figure 4c, for example, we must plot out the coincidence data collected by D_0 - D_1 and D_0 - D_2 .

Eq. 3 describes the joint wavefunction at work here. When D_1 clicks, the joint wavefunction of Eq. 3 collapses to $(-\Psi_{\gamma 1} - \Psi_{\gamma 2})$. Ignoring normalization factors, we can calculate the modulus squared as $(-\Psi_{\gamma 1} - \Psi_{\gamma 2})(-\Psi_{\gamma 1} - \Psi_{\gamma 2})^*$, where $(-\Psi_{\gamma 1} - \Psi_{\gamma 2})^*$ defines the complex conjugate. The result is:

$$|\Psi|^2 = |\Psi_{\gamma 1}|^2 + |\Psi_{\gamma 2}|^2 + 2|\Psi_{\gamma 2}||\Psi_{\gamma 1}|. \quad \text{Eq. 4}$$

Substituting ordinary plane waves $A_1 e^{i\phi_1}$ for $\Psi_{\gamma 1}$ and $A_2 e^{i\phi_2}$ for $\Psi_{\gamma 2}$ above, where A_1, A_2 are the wave amplitudes and ϕ_1, ϕ_2 are their phases, we get $(-A_1 e^{i\phi_1} - A_2 e^{i\phi_2})(-A_1 e^{-i\phi_1} - A_2 e^{-i\phi_2})$, yielding the intensity distribution of

$$I = A_1^2 + A_2^2 + 2A_1 A_2 \cos(\phi_2 - \phi_1), \quad \text{Eq. 5}$$

which describes the classic interference pattern of a double slit irradiated by a plane wave.

For the antisymmetric wavefunction, Eq. 3 collapses to $(\Psi_{\gamma 1} - \Psi_{\gamma 2})$ each time D_2 clicks. Using the same plane-wave substitutions as above, the intensity distribution looks like,

$$I = A_1^2 + A_2^2 - 2A_1 A_2 \cos(\phi_2 - \phi_1). \quad \text{Eq. 6}$$

Eq. 6 describes a double-slit pattern complementary to the one portrayed in Eq. 5. Together, Eqs. 5 and 6 mimic the patterns we see in Figure 4c. Both of these equations are didactic representations, though. Again, the actual interference patterns in the original experiment are different because of the diffraction from finite slit-widths, etc., as we saw earlier in Fig. 3 with the $\text{sinc}^2 \cos^2$ and $\text{sinc}^2 \sin^2$ plots. Nevertheless, the fundamental physics is the same.

To “see” the complementary patterns of Figure 4b, we need to plot out the coincidence data of D_0 - D_3 and D_0 - D_4 . Entangled superpositions of the orthogonally polarized photon pairs created in both regions of the BBO can be generally described in Dirac notation as

$$|\Psi\rangle = 1/\sqrt{2} [(|\Psi_{\gamma 1H}\rangle|\Psi_{\phi 1V}\rangle + |\Psi_{\gamma 1V}\rangle|\Psi_{\phi 1H}\rangle) + (|\Psi_{\gamma 2H}\rangle|\Psi_{\phi 2V}\rangle + |\Psi_{\gamma 2V}\rangle|\Psi_{\phi 2H}\rangle)], \quad \text{Eq. 7}$$

where the H and V subscripts symbolize horizontal and vertical polarization states, respectively. Eq. 7 includes both variants of the polarization states that can exist for multiple pairs of photons created in both BBO regions. For a single photon pair, this equation reduces to either

$$|\Psi\rangle = 1/\sqrt{2} (|\Psi_{\gamma 1H}\rangle|\Psi_{\phi 1V}\rangle + |\Psi_{\gamma 2H}\rangle|\Psi_{\phi 2V}\rangle) \text{ or} \quad \text{Eq. 8}$$

$$|\Psi\rangle = 1/\sqrt{2} (|\Psi_{\gamma 1V}\rangle|\Psi_{\phi 1H}\rangle + |\Psi_{\gamma 2V}\rangle|\Psi_{\phi 2H}\rangle), \quad \text{Eq. 9}$$

for the alternative orthogonal polarizations. Since the wavefunctions are orthogonal, the modulus squared of Eq. 8 becomes

$$|\Psi|^2 = 1/2 (|\Psi_{\gamma 1H}|^2 |\Psi_{\phi 1V}|^2 + |\Psi_{\gamma 2H}|^2 |\Psi_{\phi 2V}|^2), \quad \text{Eq. 10} \quad [4]$$

and the interference term that we saw in Eq. 4 vanishes. Thus, the entangled state of Eq. 8 collapses to $1/\sqrt{2} |\Psi_{\gamma 1H}\rangle|\Psi_{\phi 1V}\rangle$ if D_4 clicks, yielding a modulus squared of $1/2 |\Psi_{\gamma 1H}|^2 |\Psi_{\phi 1V}|^2$. If D_3 clicks, it collapses to $1/\sqrt{2} |\Psi_{\gamma 2H}\rangle|\Psi_{\phi 2V}\rangle$ with a modulus squared of $1/2 |\Psi_{\gamma 2H}|^2 |\Psi_{\phi 2V}|^2$. Since D_0 is scanning only the signal-photon's (γ) spatial distribution, D_0 - D_4 data therefore uncovers the clump pattern of $|\Psi_{\gamma 1H}|^2$, and D_0 - D_3 data reveals the clump pattern of $|\Psi_{\gamma 2H}|^2$ (see Figure 4b). Eq. 9 will collapse in a similar way for the alternative polarization states.

Notably, it doesn't matter whether D_0 clicks first or D_ϕ does. From the perspective of wavefunction collapse, it's just as valid to interpret a signal-photon detection collapsing the idler wavefunction as it is the other way around. The correlations between entangled states exist across spacetime. A measurement made on one quantum of an entangled pair, and the resulting simultaneous wavefunction collapse, reveals a correlation between the two quanta that is somehow independent of time and space.

Perhaps it is easier to imagine the delayed-choice quantum eraser as a game of chance played with a pair of entangled dice. Each roll of the signal die yields a random detection result, and each roll of the idler die yields another random detection result. Coincidence detections combine these two random results into a final correlated outcome. Both dice are rolled

simultaneously, but just like in a normal game of dice, it doesn't matter which die comes to rest first or even where it comes to rest. Their combined outcome is independent of the order in which each die reveals its result. So much for "retrocausality." However, unlike with a normal game of dice, if one die happens to roll out of sight, you can nevertheless infer its result by just observing the other visible die, because the two dice are entangled.

The real mystery here lies with the seemingly instantaneous connection between physically separate entangled quanta, which is why Einstein called it "spooky action at a distance." Quantum entanglement is what makes the results of this experiment, and others like it, so baffling. Feynman would be smiling.

